

Development of Test Method for Assessing the Bonding Characteristics of Membrane Layers in Wearing Course Laid on Orthotropic Steel Bridge Decks

Xueyan Liu¹, Tom Scarpas², Jinlong Li³, George Tzimiris⁴, Rob Hofman⁵, Jan Voskuilen⁶

⁽¹⁾ Corresponding author

Section of Structural Mechanics
Faculty of Civil Engineering and Geosciences, Delft University of Technology
Stevinweg 1, 2628 CN Delft, The Netherlands
Tel. +31 15 2787918
Email: X.Liu@tudelft.nl

⁽²⁾ Section of Structural Mechanics

Faculty of Civil Engineering and Geosciences, Delft University of Technology
Stevinweg 1, 2628 CN Delft, The Netherlands
Tel. +31 15 2784017
Email: A.Scarpas@tudelft.nl

⁽³⁾ Section of Structural Mechanics

Faculty of Civil Engineering and Geosciences, Delft University of Technology
Stevinweg 1, 2628 CN Delft, The Netherlands
Tel. +31 15 2784676
Email: Jinlong.Li@tudelft.nl

⁽⁴⁾ Section of Structural Mechanics

Faculty of Civil Engineering and Geosciences, Delft University of Technology
Stevinweg 1, 2628 CN Delft, The Netherlands
Tel. +31 15 2789388
Email: G.Tzimiris@tudelft.nl

⁽⁵⁾ Rijkswaterstaat, Centre for Traffic and Navigation

Schoenmakerstraat, 2628VK Delft, the Netherlands
Tel. +31 (0)887982284
Email: rob.hofman@rws.nl

⁽⁶⁾ Rijkswaterstaat, Centre for Traffic and Navigation

Schoenmakerstraat, 2628VK Delft, the Netherlands
Tel. +31 (0)887982304
Email: jan.voskuilen@rws.nl

Word Count

No. of words:	3306
No. of figures:	12*250=3000
Total:	6306

Submitted for publication and presentation for the 92nd meeting of the Transportation Research Board, 13-17 January 2013

Abstract: In order to adequately characterize the adhesive bonding strength of the various membranes with surrounding materials on orthotropic steel decks and collect the necessary parameters for FE modeling, details of the Membrane Adhesion Test (MAT) are introduced. Analytical constitutive relations of the MAT device have been derived using the same methodology as Williams (1997). Furthermore, using the experimental data obtained from MAT, ranking of the bonding characteristics of various membrane products is demonstrated as well as the role of other influencing factors, such as the types of substrate and test temperatures.

Keywords: membrane; orthotropic steel deck bridge; adhesive bonding strength; finite element; strain energy release rate

1 INTRODUCTION

2 The world-wide reported distress problems between the surfacing layers and the decks of orthotropic
3 steel bridges indicate the need for further research on the interaction between them. The severity of
4 the problem is enhanced by the considerable increase in traffic in terms of number of trucks and
5 heavier wheel loads. Innovative methodologies offer opportunities to mitigate material response
6 degradation and fatigue related problems in this type of structures thus contributing to significant
7 extension of the service life of steel bridges.

8 Preliminary investigations (1) (2) have shown that the adhesive strength of the membrane
9 layers between the surfacing layers and the decks of steel bridges has a strong influence on the
10 structural response of orthotropic steel bridge decks. The most important requirement for the
11 application of membrane materials on orthotropic steel bridge decks is that the membrane adhesive
12 layer shall be able to provide sufficient bond to the surrounding materials.

13 A number of techniques have been developed in the past to quantify the adhesive strength
14 between the membrane and the associated substrate. Among others, the blister test, initially
15 suggested by Dannenberg (3) and discussed by Gent and Lewandowski (4), is most commonly used.
16 The test specimen in the blister test consists of a perforated substrate with a thin flexible bonded
17 membrane. A fluid is injected at the interface through the perforation, thereby causing a progressive
18 debonding of the membrane. However, blister tests have several drawbacks, such as the strain
19 energy release rate increases as blister radius increases and membrane debondings become unstable.
20 The bulged area is anomalous and unpredictable especially when the substrate materials are harsh
21 and porous, for example, cement concrete or porous asphalt concrete. It is vague about the physical
22 or chemical effects of the pressurized liquid on the interface between the two bonded materials.

23 Shaft loaded blister test (SLBT), first proposed by Williams (5), is an alternative to the
24 pressured blister test. A machine driven shaft is utilized to induce central loads and displacements
25 on the membrane. Because of the slightly simpler setup and loading method, SLBT has its
26 advantages over the traditional blister test and received much attention in the last two decades. The
27 main limitation of the SLBT is about the stress singularity caused by its shaft point load. Different
28 kinds of shaft cap shapes are employed to improve this weakness. The most common way is using a
29 spherically capped shaft or ball with certain radius, (6) and (7).

30 The peel test is another commonly used method to quantify the adhesive strength of the
31 membrane to the associated substrate. However the peel test usually causes large permanent
32 deformation at the loading point, which makes the calculation of the energy release rate inaccurate.
33 The majority of mechanical energy supplied in peeling is dissipated or stored in deforming the test
34 specimen and relatively little energy actually contributes to the fracture process of the interface.

35 In the recent years, a considerable number of analytical solutions for blister tests, SLBT and
36 peel tests has been developed. The representative contributions were made by (8), (5), (9), (10) and
37 (11).

38 In order to adequately characterize the adhesive bonding strength of the various membranes to
39 surrounding materials on orthotropic steel decks and collect the necessary parameters for FE
40 modeling, a Membrane Adhesion Test (MAT) device has been developed by the Delft University of

41 Technology. The innovative MAT device has several advantages. By using a cylindrical loading
42 piston head, the piston force can be applied uniformly on the membrane surface with negligible
43 boundary effects. The cylindrical loading piston heads designed with different radii are optional to
44 minimize damage on the test membrane so that the reliability of test results is guaranteed. From the
45 relatively simple analytical solution of the constitutive relation, the energy release rate and
46 membrane strain expressions can be derived. A laser scanning system is utilized to measure
47 membrane deformation, capturing the membrane deformation profile over time.

48 In this paper, details of the MAT test are introduced to characterize the adhesive characteristics of
49 the various membranes with the surrounding materials. Analytical constitutive relations of the MAT
50 device have been derived using the same methodology as Williams (1997). Furthermore, on the
51 basis of experimental data obtained from the MAT device, ranking of the bonding characteristics of
52 different membrane products is demonstrated as well as the role of other influencing factors, such as
53 the substrate type and test temperature. Availability of the MAT results will allow a better
54 understanding of performance of the membrane allowing optimization of maintenance activities.

55 **APPARATUS**

56
57 The MAT test system consists of a loading device, an environmental chamber, laser scanning
58 device and a data acquisition system. The loading device includes a computer controlled loading
59 component which, during each loading cycle, in response to commands from the data processing and
60 control component, adjusts and applies a load on the tested membrane. The loading device is
61 capable of (1) providing repeated haversine loading at a frequency range of 0 Hz to 12 Hz, (2) lifting
62 the piston to the maximum height of 130 mm after the piston comes to contact with the test
63 membrane, (3) providing a maximum force up to 5 kN, (4) providing two piston heads with radius
64 of 90mm and 75mm. Figure 1 illustrates the components of the MAT device.

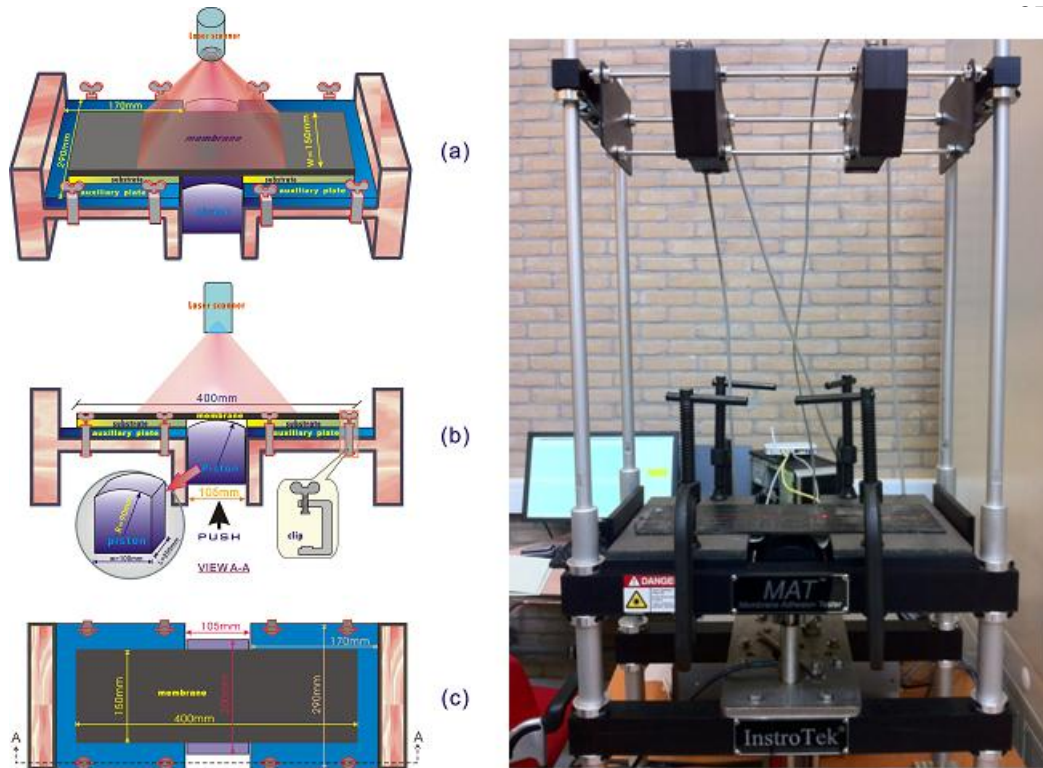
65 The laser scanning system senses the shape of the deformed object and collects data that
66 defines the location of the outer surface of the membrane. A line laser is utilized to measure the
67 membrane deformation profile over time across 150 mm width. The laser scanner can be operated in
68 a temperature range from -10°C to 55°C. The frequency of the laser scanner is up to 250Hz for the
69 full range.

70 An environmental chamber is utilized to enclose the entire test set up and maintains the
71 specimen at controlled temperature. The environmental chamber is not required if the temperature of
72 the surrounding environment can be maintained within the specific limits. The chamber can provide
73 temperature range of -15°C to 80°C and relative humidity range of 10% to 95%.

74 During each load cycle the control and data acquisition system are capable of measuring the
75 load and deformation of the piston and adjusting the load or displacement applied by the loading
76 device and the loading frequency. In addition, it is capable of recording load cycles, applied loads,
77 and piston deformations.

78 In this paper, details of the MAT test have been introduced to characterize the adhesive
79 characteristics of the various membranes with the surrounding materials. Analytical constitutive

80 relations have been derived for the MAT device. Furthermore, on the basis of experimental data
 81 obtained using the MAT device, ranking of the bonding characteristics of different membrane
 82 products is demonstrated as well as the role of other influencing factors, such as the substrate type
 83 and test temperature. Availability of the MAT results will allow a better understanding of
 84 performance of the membrane allowing thus optimization of maintenance activities.
 85
 86



108
 109 **FIGURE 1 Schematic of MAT device**

110
 111
 112 **SPECIMEN PREPARATION**

113
 114 In the Netherlands an asphaltic surfacing structure for orthotropic steel bridge decks mostly consists
 115 of two structural layers. The upper layer consists of Porous Asphalt (PA) because of reasons related
 116 to noise hindrance. For the lower layer a choice between Mastic Asphalt (MA) or Guss Asphalt
 117 (GA), can be made, see Figure 2. In order to characterize the adhesive bonding strength of various
 118 membrane products utilized in the Dutch steel deck bridges, three types of specimen, i.e. steel-
 119 membrane specimen (SM), Guss Asphalt Concrete-membrane specimen (GM) and Porous Asphalt-
 120 membrane specimen (PM), are included in this research project.
 121

122
 123
 124
 125
 126
 127
 128
 129
 130
 131
 132
 133
 134
 135
 136
 137
 138
 139
 140
 141
 142
 143
 144
 145
 146
 147
 148
 149
 150
 151
 152
 153
 154
 155
 156
 157
 158
 159
 160
 161
 162
 163

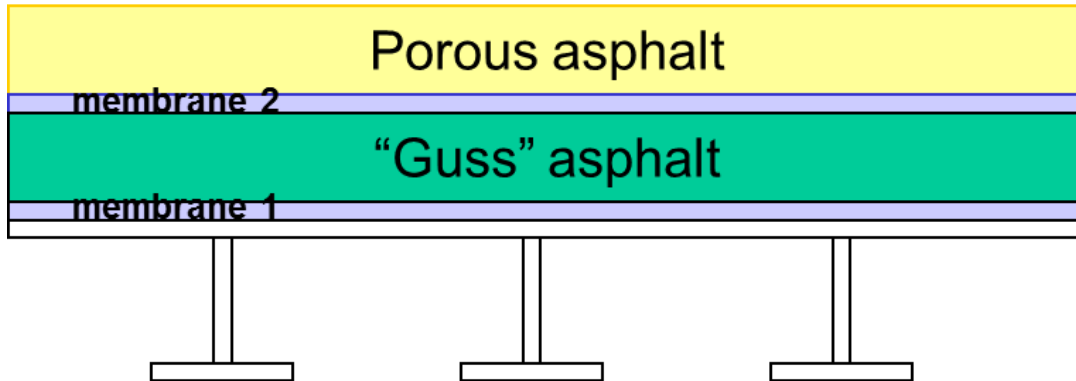


Figure 2 Schematic of a typical Dutch asphalt surfacing system on a steel bridge

For the SM specimen preparation, two pieces of square steel plates with thickness 6 mm is used. The steel plate shall be cleaned in accordance with EN ISO 8503-1. The membrane with dimension t is the thickness of the tested membrane shall be bonded to the steel plate in accordance with standard procedures provided by membrane manufacturers.

Because the GM system consists of two interfaces, one is the membrane on the bottom of the guss asphalt (named GM1) and another is the membrane on the top of the guss asphalt (named GM2). Therefore two types of GM specimens shall be prepared. Due to the physical characteristics of Guss asphalt, a mould shall be utilized for preparation of GM specimens. The procedures of installation of membrane on top or bottom of the guss asphalt shall be according to the membrane manufacture specification.

For the preparation of PM specimen, a mould is utilized. The PM specimen dimension is 400mm by 150mm by 40mm. The porous asphalt is compacted on top of the membrane. After compaction, the porous asphalt requires a minimum curing time of 14 days and a maximum of 8 weeks before testing. Porous asphalt preparation shall be performed in accordance with NEN-EN 12697-33.

CONSTITUTIVE RELATIONS

In order to derive the constitutive relations of the MAT test, a deformed thin membrane with thickness h and width b is shown in Figure 4. A central load, F is applied to the membrane via a cylindrically capped piston with radius, R . The deformed height of the centre point at the outer surface of the membrane is H . There are two contact situations that may occur in the MAT tests. The first situation is that the piston partially contacts the membrane, see Figure 3. The second situation is the membrane contacts fully to the piston and the membrane will be stretched in straight after the kinks of the piston touch to the membrane, see Figure 4.

164
165
166
167
168
169
170
171
172
173
174
175
176
177
178
179
180
181
182
183
184
185
186
187
188
189
190
191
192
193
194

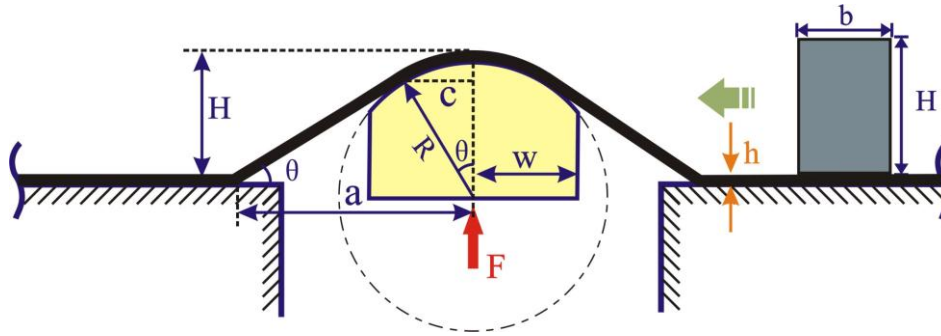


FIGURE 3 Cylindrically capped MAT (membrane contacts partially to the piston head)

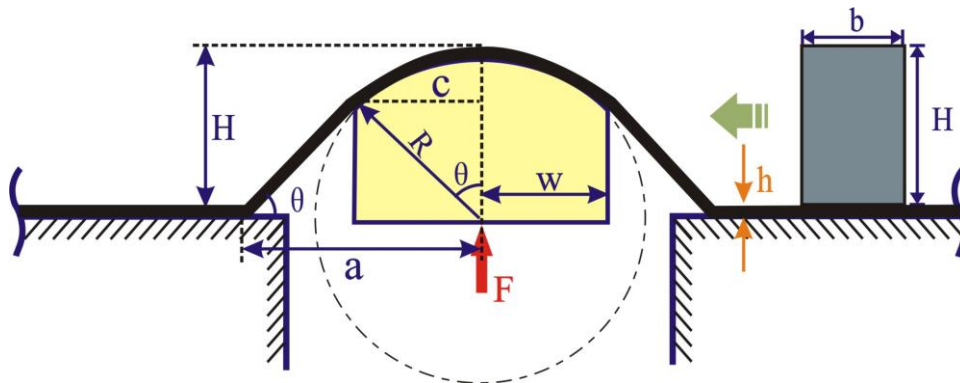


FIGURE 4 Cylindrically capped MAT (membrane contacts fully to the piston head)

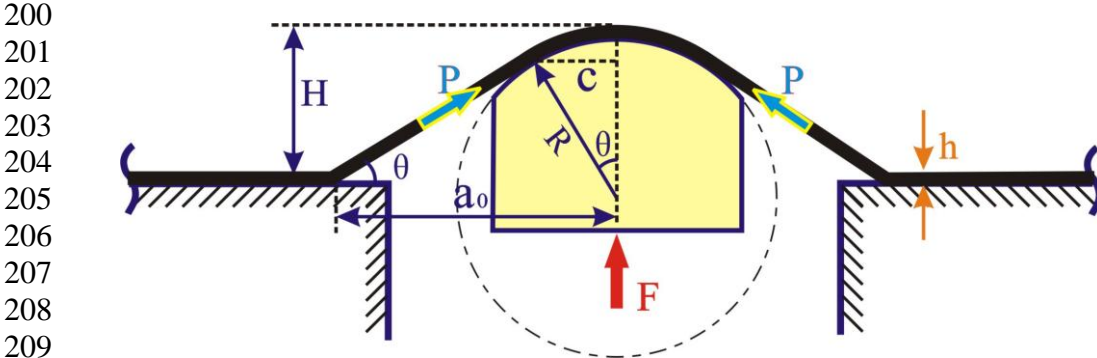
The complete solutions of the load point height H and the membrane strain, ε are summarized by the combinations of the aforementioned two contact situations:

$$H = \begin{cases} a \tan \theta - R \left(\frac{1 - \cos \theta}{\cos \theta} \right) & \left(\sin \theta \leq \frac{W}{R} \right) \\ (a - W) \tan \theta + R - \sqrt{R^2 - W^2} & \left(\sin \theta > \frac{W}{R} \right) \end{cases} \quad (1)$$

195

$$\varepsilon = \begin{cases} \left(\frac{1 - \cos \theta}{\cos \theta} \right) + \frac{R}{a} (\theta - \tan \theta) & \left(\sin \theta \leq \frac{W}{R} \right) \\ \left(\frac{1 - \cos \theta}{\cos \theta} \right) - \frac{w}{a \cos \theta} + \frac{R \theta_0}{a} & \left(\sin \theta > \frac{W}{R} \right) \end{cases} \quad (2)$$

196
 197 where the notations in equations (1) and (2) are indicated in Figure 3 and Figure 4.
 198 In order to derive the relationship between actuator load F and the membrane strip angle θ , a
 199 schematic of force resolution for MAT is illustrated in Figure 5.



210 **FIGURE 5 Force resolution for MAT**

211
 212 Force along membrane strip is:

$$P = \frac{F}{2 \sin \theta} = \sigma b h \quad (3)$$

213
 214 Actuator load F becomes:
 215

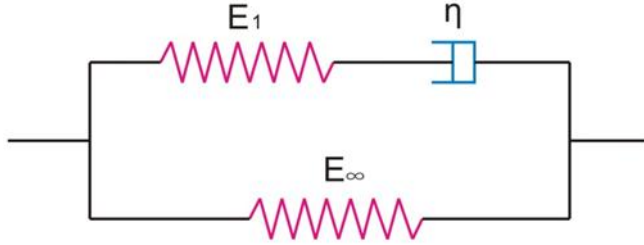
$$F = 2 \sigma b h \sin \theta \quad (4)$$

216
 217 Furthermore, for an elastic membrane, the actuator load for the aforementioned two contact
 218 situations can be expressed by:

$$F = 2bh\sigma \sin \theta = \begin{cases} 2bh \sin \theta E \left[\left(\frac{1 - \cos \theta}{\cos \theta} \right) - \frac{R}{a} (\tan \theta - \theta) \right] & \left(\sin \theta \leq \frac{W}{R} \right) \\ 2bh \sin \theta E \left[\left(\frac{1 - \cos \theta}{\cos \theta} \right) - \frac{W}{a \cos \theta} + \frac{R\theta_0}{a} \right] & \left(\sin \theta > \frac{W}{R} \right) \end{cases} \quad (5)$$

219 However, for bridge construction, the membranes products which are utilized for MAT test are
 220 mostly made by bitumen-based materials, thereby the mechanical responses of the membrane
 221 material are time dependent and temperature sensitive. In order to study the membrane response
 222 properly, membrane has to be treated as a visco-elastic material. In this investigation, Zener model is
 223 utilized for computing the stress σ in equation (4).

224 For sake of convenience, Figure 6 shows the mechanical analog of visco-elastic Zener model.
 225



226
227

228 **FIGURE 6 Schematic of Zener model**

229

230 The model consists of two parallel components. One is purely elastic with modulus E_∞ and the
231 other is viscoelastic consisting of a spring with modulus E_1 and a damper with viscosity coefficient
232 η in series.

233 The total applied stress σ can be decomposed in two components. one is the stress σ_1 in the
234 viscoelastic component and the other is the stress σ_2 in the elastic component. It can be expressed as:

$$\begin{aligned}\sigma &= \sigma_1 + \sigma_2 = E_\infty \varepsilon + E_1 (\varepsilon - \varepsilon_v) \\ E_1 (\varepsilon - \varepsilon_v) &= \eta \dot{\varepsilon}_v\end{aligned}\quad (6)$$

235 in which $\varepsilon_v = \varepsilon(t) - \varepsilon(0) \exp\left(-\frac{E_1}{\eta} t\right) - \int_0^t \exp\left(-\frac{E_1}{\eta} (t-\tau)\right) \dot{\varepsilon}(\tau) d\tau$ is viscous strain of membrane

236 and $\varepsilon(0)$ is the initial strain at time zero.

237

238 STRAIN ENERGY RELEASE RATE

239

240 The strain energy release rate G_c characterizes the energy per unit crack or debonding area required
241 to extend, and as such is expected to be the fundamental physical quantity controlling the behavior
242 of the material bonding strength. Considering a membrane adhered to a substrate as shown in Figure
243 4, using a Griffith argument (12), the general definition of energy release rate can be expressed by:

244

$$G = \frac{d}{dA} [U_{\text{ext}} - U_s - U_d - U_k] \quad (7)$$

245

246 where U_{ext} is the external work; U_s is the strain energy; U_d is the dissipated energy; U_k is the kinetic
247 energy; A is the area create.

248 By considering a strip membrane bonded to a substrate surface and debonded over a length
249 $2a$ in Figure 7, H , a and θ change during membrane debonding but with the continuity condition the
250 sloping length $2s$ is increased such that $ds=da$. Now that $a=s \cdot \cos\theta$ and $H=s \cdot \sin\theta$, i.e.

251

$$\frac{da}{d\theta} = \frac{ds}{d\theta} \cdot \cos\theta - s \cdot \sin\theta = -\frac{s \sin\theta}{1 - \cos\theta} \quad (8)$$

252

also

$$\frac{dH}{d\theta} = \frac{ds}{d\theta} \cdot \sin \theta + s \cdot \cos \theta = -s \quad (9)$$

253 hence

$$\frac{dH}{da} = \frac{1 - \cos \theta}{\sin \theta} \quad (10)$$

254

255

256

257

258

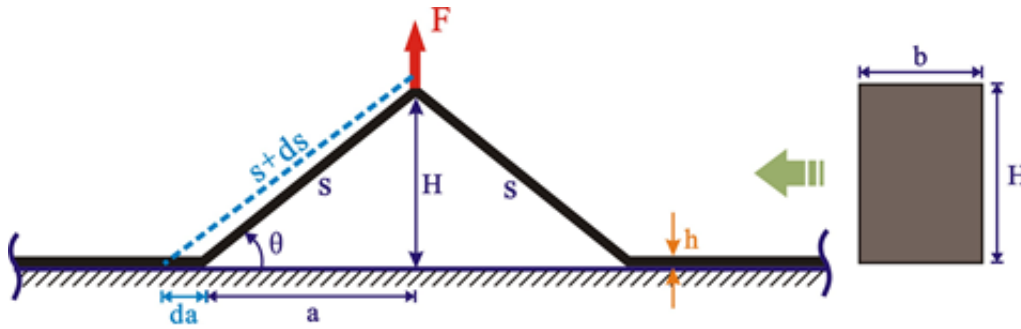
259

260

261

262

263



264 **FIGURE 7 Schematic of debonded membrane strip**

265

266

267

According to Williams [10], for a flexible but inextensible membrane strip with a slow peeling load, the strain energy release rate becomes:

$$G = \frac{dU_{\text{ext}}}{2bda} = \frac{F \cdot dH}{2bda} = \frac{F}{2b \sin \theta} (1 - \cos \theta) \quad (11)$$

268

269

270

For linear elastic and extensible membrane strip in Figure 7, the energy release rate in Eq. (11) can be written by:

$$G = \frac{F}{2b \sin \theta} \left(1 - \cos \theta + \frac{\varepsilon}{2} \right) \quad (12)$$

271

272

By substituting Eq. (2) into (12), the strain energy release rate G of MAT test becomes:

$$G = \begin{cases} \frac{F(a \cos \theta - 2a \cos^2 \theta + a + R\theta \cos \theta - R \sin \theta)}{4ab \sin \theta \cos \theta} & \left(\sin \theta \leq \frac{W}{R} \right) \\ \frac{F(a \cos \theta - 2a \cos^2 \theta + a + R\theta_0 \cos \theta - W)}{4ab \sin \theta \cos \theta} & \left(\sin \theta > \frac{W}{R} \right) \end{cases} \quad (13)$$

273

274

275

276

277

278

279

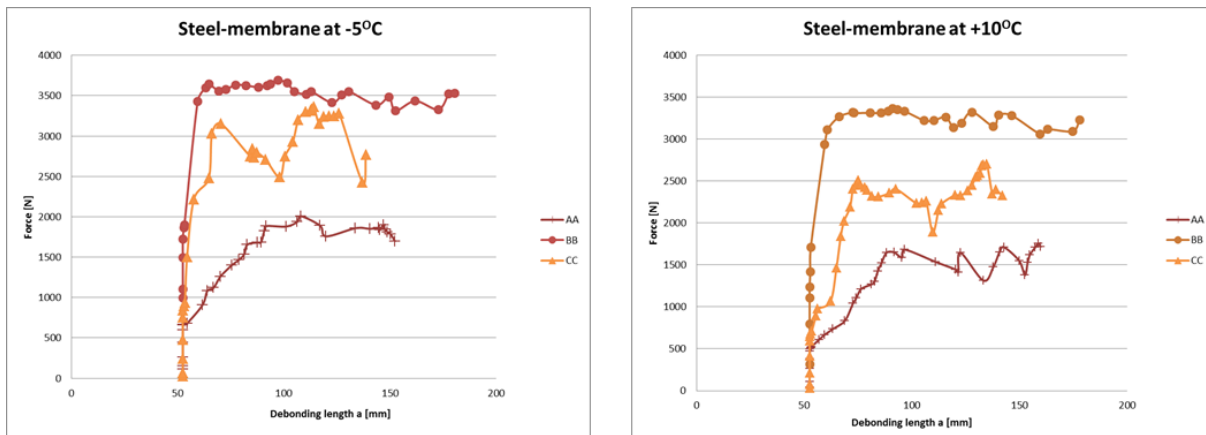
Since the actuator load F and membrane strip angle θ in equation. (13) can be measured directly via MAT device, the critical value of $G=G_c$ can be determined when the membrane starts to debond.

RESULTS AND DISCUSSIONS

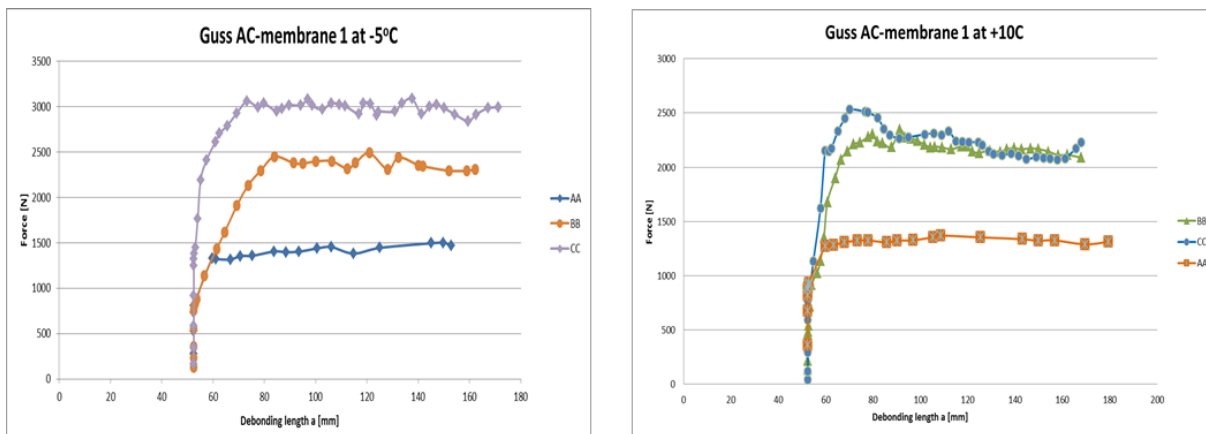
280 In this paper, MAT monotonic test results of three different membranes indicated by AA, BB and
 281 CC bonded with three different substrates (Steel, Guss asphalt and Porous asphalt) are presented. To
 282 determine the role of ambient temperature, the tests were performed over the range of temperatures -
 283 5°C to +10°C.

284 Figure 8 through Figure 11 show the variations of piston reaction force obtained by the MAT
 285 device versus the membrane debonding length. The following observations are made:

- 286 • The mechanical response of membrane product is influenced not only by the surrounding
 287 substrate but also by the environmental temperature;
- 288 • Initially the piston reaction force increases linearly. In most cases there is either a
 289 gradually increasing non-linearity or sudden crack extension and arrest (called ‘pop-in’)
 290 followed by non-linearity;
- 291 • In most cases, product BB shows a higher reaction force development than the product
 292 AA and CC;
- 293 • All products within SM, GM1 and PM samples show a higher reaction force at lower
 294 temperature except the one within GM2 samples;

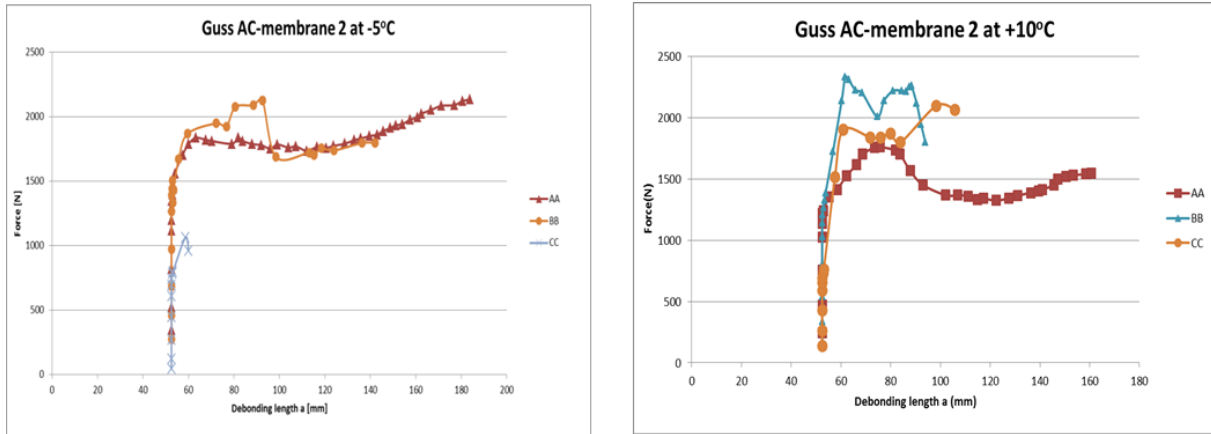


296
 297 **FIGURE 8 Force versus debonded length of SM samples**

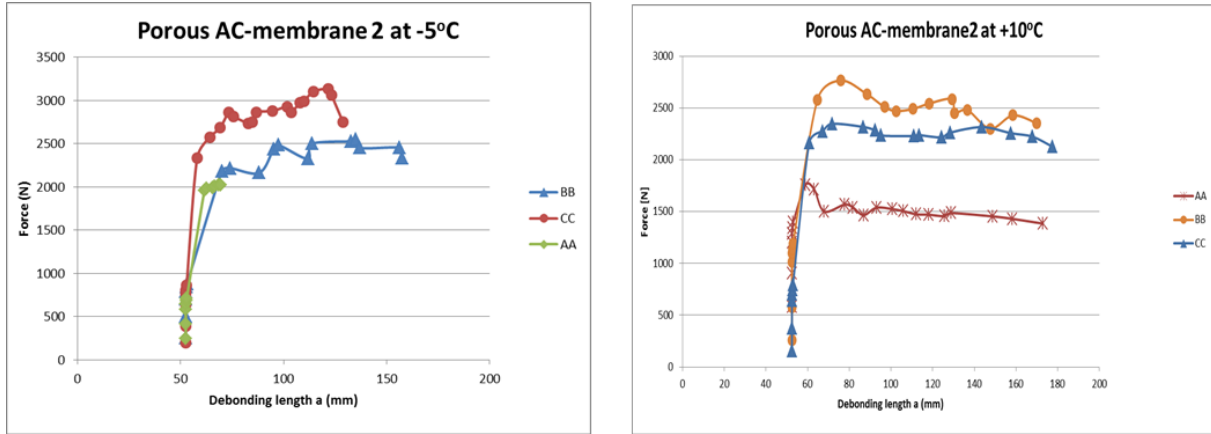


298
 299

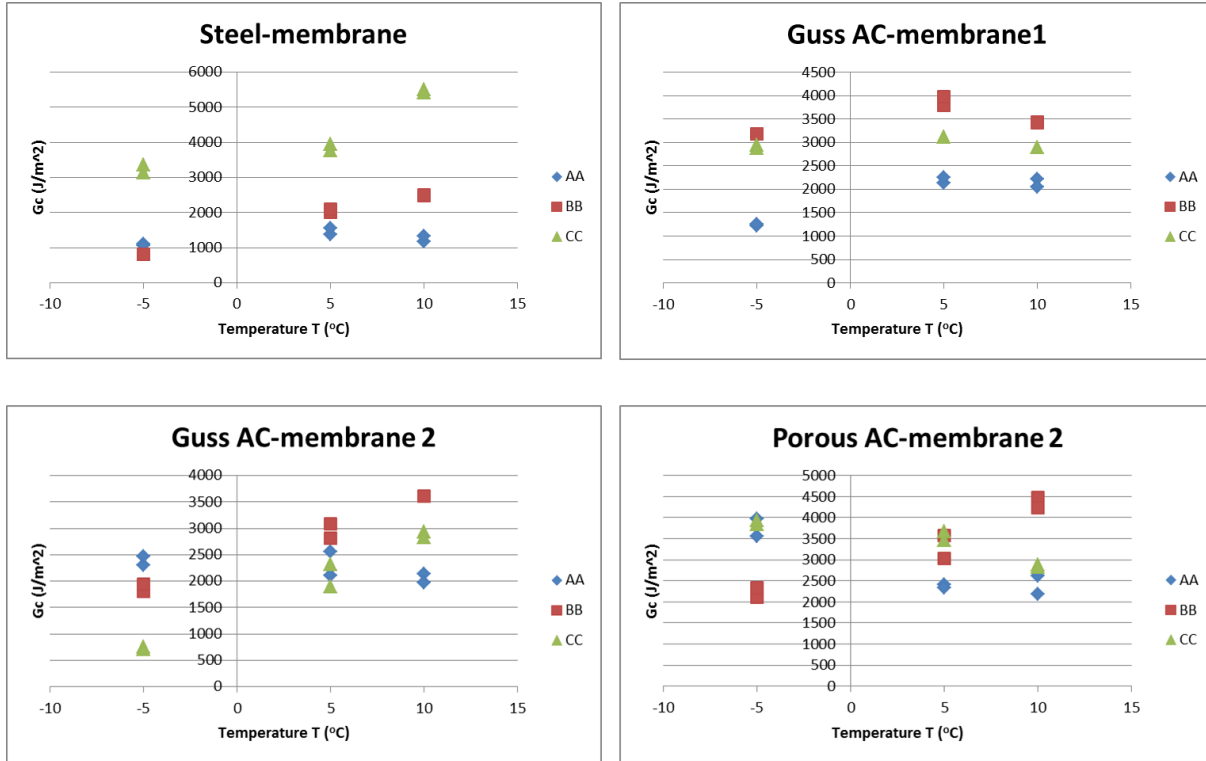
300 **FIGURE 9 Force versus debonded length of GM1 samples**
301



304 **FIGURE 10 Force versus debonded length of GM2 samples**
305



308 **FIGURE 11 Force versus debonded length of PM2 samples**



309
 310
 311
 312
 313
 314
 315
 316
 317
 318
 319
 320
 321
 322
 323
 324
 325
 326
 327
 328
 329
 330
 331

FIGURE 12 Comparison of strain energy release rate among different samples

Figure 12 gives the comparison of critical strain energy release rate, G_c among different samples over the range of temperatures -5°C , $+5^{\circ}\text{C}$ and $+10^{\circ}\text{C}$. The following observations and conclusions are made

- The bonding strength of membrane products depends on both the characteristic properties of the substrate material and the environmental temperature;
- In general, product BB with GM and PM samples gives higher G_c at all test temperatures. Product AA and CC with PA samples show G_c values decreasing with an increase in temperature. Product CC with SM and GM2 samples shows increasing G_c values with temperature; Products AA, BB and CC with GM1 samples show a higher G_c at $+5^{\circ}\text{C}$;
- By comparing Figure 12 with Figure 8 through Figure 11, it can be observed that higher maximum piston reaction force does not necessarily result in higher G_c values. This inconsistency may occur due to the fact that maximum piston reaction force represents both membrane material response and membrane bonding characteristics. However G_c is a physical material quantity controlling the behavior of only the membrane bonding strength;

CONCLUSIONS AND RECOMMENDATIONS

Based on the results presented in this paper, the following conclusions and recommendations can be made.

1. The MAT setup is capable of characterizing the adhesive bonding strength of the various membranes with the surrounding materials. MAT results will allow a better understanding of performance of the membrane on the bridge structure thus allowing optimization of maintenance activities;
2. Critical strain energy release rate G_c is a fundamental physical quantity that can be utilized to quantify the membrane adhesive bonding strength with different substrates;
3. The bonding strength of the membrane product depends both on the material characteristics of substrate material and the environmental temperature;
4. In the near future, the MAT cyclic load test will be developed to characterize the membrane fatigue life. The influence of the material non-linearity on membrane adhesive strength and fatigue life shall be studied further.

ACKNOWLEDGEMENT

This work is part of the research program of InfraQuest. InfraQuest is a collaboration between Rijkswaterstaat, TNO and the Delft University of Technology. This research project is partially funded by the Dutch Transport Research Centre (DVS) of the Ministry of Transport, Public Works and Water Management (RWS). Their financial support is highly appreciated..

REFERENCES

1. Liu, X., Medani, T. O., Scarpas, A., Huurman, M. and Molenaar, A. A. A., Experimental and numerical characterization of a membrane material for orthotropic steel deck bridges: Part 2 - Development and implementation of a nonlinear constitutive model, *Finite Elements in Analysis and Design*, vol. 44, pp. 580-594, 2008.
2. Medani, T. O. , Design principles of surfacings on orthotropic steel bridge decks, *PhD, Delft University of Technology*, Delft, 2006.
3. Dannenberg, H., Measurement of Adhesion by a Blister Method, *J. Appl. Polym. Sci.*, vol. 33, pp.509-510, 1958.
4. Gent, A. and Lewandowski, L., Blow-Off Pressures for Adhering Layers, *J. Appl. Polym. Sci.*, vol 33, pp.1567 -1577, 1987.
5. M.L.Williams, The continuum interpretation for fracture and adhesion, *Journal of Applied Polymer Science*, vol. 13, pp. 12, 1969.
6. Liao, K. & Wan, K. T., Evaluation of film-substrate interface durability using a shaft-loaded blister test, *J. Compos Tech Res*, vol. 23, pp.15-20, 2001.

- 370 7. Xu, X. J., Shearwood, C. & Liao, K., A shaft-loaded blister test for elastic response and
371 delamination behavior of thin film-substrate system, *Thin Solid Films* vol.424, pp.115-119,
372 2003.
- 373 8. Malyshev, B.M. & Salganik, R.L., The strength of adhesive joints using the theory of cracks,
374 *International Journal of Fracture Mechanics*, vol.1, pp.15, 1965.
- 375 9. Storakers, B. & Andersson, B., Nonlinear Plate-Theory Applied to Delamination in Composites,
376 *J Mech Phys Solids*, vol.36, pp.689-718, 1988.
- 377 10. Williams, J. G., Energy release rates for the peeling of flexible membranes and the analysis of
378 blister tests, *Int J Fracture* vol.87, pp.265-288, 1997.
- 379 11. Jin, C. Analysis of energy release rate and bending-to-stretching behavior in the shaft-loaded
380 blister test, *Int J Solids Struct* vol.45, pp.6485-6500, 2008.
- 381 12. Kanninen, M. F. & Poplar, C. H., *Advanced Fracture Mechanics*, Oxford University Press,
382 Chapter 3, 1985.
- 383
384
385